arXiv:1702.04412v1 [cond-mat.quant-gas] 14 Feb 2017

Emergence of the $\rho = 1$ Mott lobe in an anyon chain with three-body interactions

J. Arcila-Forero, R. Franco, and J. Silva-Valencia*
Departamento de Física, Universidad Nacional de Colombia, A. A. 5997 Bogotá, Colombia.
(Dated: February 16, 2017)

A quantum phase transition driven by the statistics was observed in an anyon-Hubbard model with local three-body interactions. Using a fractional Jordan-Wigner transformation, we arrived at a modified Bose-Hubbard model, which exhibits Mott insulator and superfluid phases. The absence of a Mott insulator state with one particle per site depends on the anyonic angle, and a quantum phase transition from a superfluid to a Mott insulator state is obtained for a fixed value of the hopping. The critical points were estimated with the von Neumann block entropy and increase as the hopping grows. The statistics modify the ground state, and three different superfluid regions were observed for larger values of the anyonic angle.

I. INTRODUCTION

Commonly, particles in quantum theory are classified into two types, bosons and fermions, depending on their particle exchange characteristics. For two bosons, the wavefunction remains invariant under particle exchange, whereas the exchange of two fermions leads to a multiplicative factor -1 in the wavefunction. Physicists have proposed a third class of particles with nontrivial exchange statistics, anyons, particles carrying fractional statistics that interpolate between bosons and fermions [1–3]. For two anyons under particle exchange, the wave function acquires a fractional phase $e^{i\theta}$, giving rise to fractional statistics with $0 < \theta < \pi$. Quickly it was found that relevant quantum phenomena can be explained in terms of these new particles, the fractional quantum Hall effect [4–7] being the best known, and nowadays it is believed that anyons will be important in condensed matter physics and topological quantum computation [8–10].

The study of anyons was restricted for many years to two-dimensional systems. However, with Haldane's definition of fractional statistics, it was generalized to arbitrary dimensions [3]. Anyons in one dimension (1D) have been widely studied, their commutation relations [11], dispersion relations and the dependence between generalized exclusion statistics and the anyonic angle [12], correlation functions in the low-momentum regime [13], the dynamical properties in a weak harmonic trap [14], the ground state properties of hard-core anyons [15], and mixtures of anyons under an external trap [16] having been found. Also, it has been observed that the excitations of some one-dimensional models can be explained in terms of anyons [17, 18].

The creation and manipulation of physical setups that display fractional statistics is a huge challenge for experimental physicists, although several proposals have been made [19–24]. One of the most popular approaches for observing fractional physics is to confine ultracold bosonic atoms in an optical lattice, whose requirements have been considerably changed and simplified recently [25–27]. The anyon-Hubbard model, which takes into account the kinetic energy of the anyons and the local two-body repulsion between them, arises from the above proposals. The ground state and the phase diagrams as a function of the tunelling, the local interaction, and the statistics have been studied using mean field theory and the density matrix renormalization group method [25, 28, 29]. In others studies, the quasimomentum distribution [30], the one-body reduced density matrix in a harmonic potential [31] and a nontrivial topological Haldane phase were explored [32].

In the experimental setups of cold atoms using optical lattices, it is possible to tune the tunelling parameter of particles in a lattice, the interaction strength through Fesbash resonance, the density of particles, and the dimensionality, and for this reason they have emerged as unusual laboratories for the realization of boson- and fermi-Hubbard models, as well as for observing phase transitions without the intrinsic uncertainty posed by materials [33, 34]. Also, these setups have allowed the observation of many-body interaction effects [35, 36], stimulating new experimental proposals and theoretical calculations about the physical properties of bosonic systems with relevant three-body interactions between particles [37–40].

An unexplored problem consists of considering delocalized anyons in a one-dimensional optical lattice under local three-body interactions. This problem it is interesting because the three-body interactions between spinless or spinor bosons cannot generate a Mott insulator state with one particle per site and also change the phase diagram. On the other hand, it has been shown that the anyonic statistics localize the particles, and this can induce a quantum phase transition in systems with two-body interactions. In the present paper, we study the interplay between the above phenomena and write a Hamiltonian with two terms: the local three-body interaction and the kinetic energy. Using a fractional Jordan-Wigner transformation, this Hamiltonian was mapped to a modified Bose-Hubbard Hamiltonian with the tunneling depending on the local density and local three-body interactions, which will be studied numerically. The ground state can be superfluid or Mott insulator, in accordance with our

* jsilvav@unal.edu.co

density matrix renormalization results for finite lattices. We build two phase diagrams, the chemical potential as a function of the statistical angle for a fixed hopping parameter and the chemical potential versus the hopping for a fixed anyonic angle. We found that an increase in the statistical angle generates a Mott insulator state with one anyon per site; therefore, a superfluid-Mott insulator transition driven by the statistics was observed. We expect that this quantum phase transition will be observed in the near future when recent proposals for creating an anyon system and obtaining a regime where the three-body interaction domain are realized. We would like to point out that a pior report on the interplay between many-body effects and anyonic statistics had been made [41].

Our study is organized in the following way: The anyon-Hubbard model with local three-body interactions is explained in Sec. I A. Using the von Neumann block entropy and the excitation gap in sec. I B, we distinguish the quantum phases of the model and draw the phase diagrams of the model. Finally our main findings and final comments appear in Sec. I C.

A. Model

In one dimension, the operators of creation ($a_j^\dagger$) and annihilation (a_j) of an anyon at site j satisfy the following commutation relations:

$$\begin{aligned} a_j a_k^\dagger - e^{-i\theta sgn(j-k)} a_k^\dagger a_j = \delta_{jk}, \\ a_j a_k - e^{i\theta sgn(j-k)} a_k a_j = 0, \end{aligned} \tag{1}$$

where θ denotes the statistical phase, and the sign function (multistep function) is $sgn(j-k) = \pm 1$ for $j > k$ and $j < k$, and $sgn(j-k) = 0$ for $j = k$. Note that, two particles on the same site reproduce the ordinary bosonic commutations relations.

The quantum phases of a set of soft-anyons is a subject of great interest at this moment, and they come from the interplay between the hopping of the carries throughout the lattice and the interactions. In the present paper, we consider repulsive local three-body interactions, and the Hamiltonian is given by

$$\begin{aligned} H = -t \sum_j^{L-1} \left(a_j^\dagger a_{j+1} + h.c. \right) \\ + \frac{W}{6} \sum_j^L n_j (n_j - 1)(n_j - 2), \end{aligned} \tag{2}$$

$t > 0$ being the tunneling amplitude connecting two neighboring sites, W the on-site interaction, L the length of the lattice, and n_j the number operator. The first term in the Hamiltonian (2) is the kinetic energy with strength t, and the second term stems from the short-range interaction between three particles. Our unit of energy will be $W = 1$ unless otherwise specified.

The fractional version of the Jordan-Wigner transformation

$$a_j = b_j \; exp\left(i\theta \sum_{i=1}^{j-1} n_i \right), \tag{3}$$

defined by Keilmann *et al.* establishes an exact mapping between anyons and bosons in one-dimension [25]. Here, the operator b_j describes spinless bosons, which satisfy $[b_j, b_i^\dagger] = \delta_{ji}$ and $[b_j, b_i] = 0$. Note that the representation of the number operator in terms of anyon or boson operators is the same ($n_i = a_i^\dagger a_i = b_i^\dagger b_i$).

Applying the anyon-boson mapping (3) to the anyon-Hubbard Hamiltonian with three-body interaction (2), we obtain a Hamiltonian in terms of boson operators, which allows us to explore the ground state, but also establishes a link between the anyon-Hubbard Hamiltonian with its possible experimental realization in cold atoms setups. Therefore the bosonic version of the anyon-Hubbard Hamiltonian with three-body interaction is given by

$$\begin{aligned} H = -t \sum_j^{L-1} \left(b_j^\dagger b_{j+1} e^{i\theta n_j} + h.c. \right) \\ + \frac{W}{6} \sum_j^L n_j (n_j - 1)(n_j - 2). \end{aligned} \tag{4}$$

In this way, the above Hamiltonian describes bosons with the tunneling depending on the local density $te^{i\theta n_j}$ for hopping processes from right to left ($j + 1 \to j$). All of the influence of the fractional statistics is concentrated in this term. If the target site j is unoccupied, the hopping amplitude is simply t. If it is occupied by one boson, the amplitude reads $te^{i\theta}$, for two bosons $te^{i2\theta}$, and so on.

B. Results

Nowadays it is well known that quantum information tools are useful for distinguishing different quantum phases, and also we can estimate the border or critical point that separates one region from another, although there is no "universal" measure of entanglement that works for any quantum problem [42]. Despite the relevance emphasized by many people and the possible applications of entanglement in diverse areas of physics, experiments for directly detecting and measuring the degree of entanglement of a system are challenging for science. Recently, in an experiment with atoms confined in optical lattices, it was possible to measure the quantum purity, Rényi entanglement entropy, and mutual information of a Bose-Hubbard system [43]. These results reinforced the connection between quantum information tools and the description of degenerate gases realized in cold atom setups.

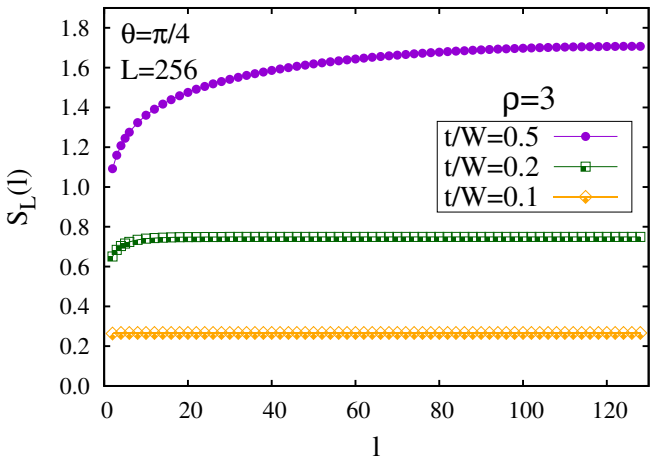

FIG. 1. The von Neumann block entropy $S_L(l)$ as a function of l for an anyon chain with $\theta = \pi/4$, $\rho = 3$ and size $L = 256$. Here we consider three different values of the hopping parameter, $t/W = 0.1, 0.2$, and 0.5. Clearly, we can see that a change of state happens as the hopping grows.

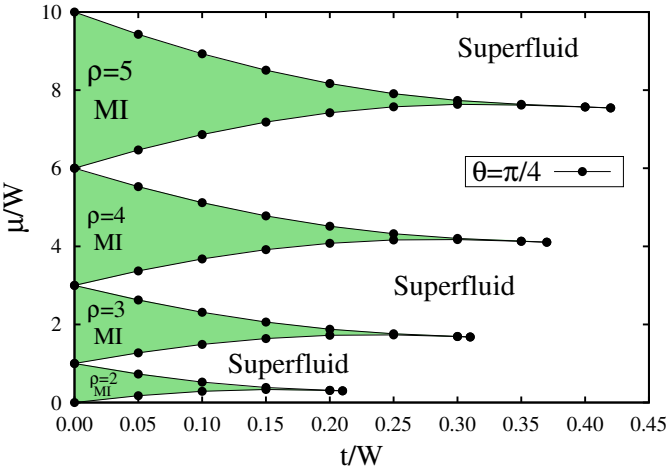

FIG. 2. Phase diagram of the anyon-Hubbard model with local three-body interactions for $\theta = \pi/4$ and for the densities $\rho = 2, 3, 4$ and 5. The points correspond to extrapolations to the thermodynamic limit from DMRG data and the lines are visual guides. MI means Mott insulator regions.

Bipartite measures of entanglement are the most used. Therefore, we consider a system with L sites divided into two parts. Part A has l sites ($l = 1, ..., L$), and the rest form part B, with $L - l$ sites. The von Neumann block entropy of block A is defined by $S_A = -Tr\varrho_A ln\varrho_A$, where $\varrho_A = Tr_B\tilde{\varrho}$ is the reduced density matrix of block A and $\tilde{\varrho} = |\Psi\rangle\langle\Psi|$ the pure-state density matrix of the whole system. For a system with open boundary conditions, the behavior of the von Neumann block entropy as a function of l depends on the nature of the ground state and provides information about the type of phase, because it saturates (diverges) if the system is gapped (gapless) [44]. Thus:

$$S_L(l) = \begin{cases} \frac{c}{6} ln[\frac{2L}{\pi} sin(\frac{\pi l}{L})] + \Theta, & \text{critical,} \\ \\ \frac{c}{6} ln[\xi_L] + \Theta', & \text{non critical,} \end{cases} \quad (5)$$

c being the central charge and ξ_L the correlation length. The constants Θ and Θ' are nonuniversal and model dependent.

To determine the ground state wave function ($|\Psi\rangle$) of a lattice with L sites and N particles, we used the finite-size density matrix renormalization group algorithm (DMRG) with open boundary conditions, and in order to improve the calculations, we implemented the dynamical block state selection (DBSS) protocol based on a fixed truncation error of the subsystems reduced density matrix instead of using a fixed number of preserved states in the DMRG sweeps [45]. Also, we truncated the local Hilbert space by considering only $\rho + 5$ states when the density of the particles is $\rho = N/L$ [46]. With the above considerations, we obtained a discarded weight of around 10^{-10} or less, and the maximum number of states maintained was $m = 1200$.

The evolution of the von Neumann block entropy $S_L(l)$ as the size of the block increases is shown in Fig. 1 for a lattice with global density $\rho = 3$, statistical angle $\theta = \pi/4$, and three different values of the hopping: $t/W = 0.1$, $t/W = 0.2$, and $t/W = 0.5$. For small values of the hopping parameter, we expected that the particles would tend to localize and the entanglement would be small. This happened for $t/W = 0.1$, and we observed that the von Neumann block entropy saturates very quickly and has a small value. The above behavior continues for larger values of the hopping parameter ($t/W = 0.2$), but the maximum numerical value is larger, indicating that the entanglement has increased. These results indicate that for a wide range of values of the hopping the system remains in a phase characterized by a finite correlation length, in accordance with the expression Eq. (5). However, things change for larger values. For $t/W = 0.5$, the von Neumann block entropy increases smoothly and tends to diverge with the block size, which characterizes a critical state. In this way, the calculation of the von Neumann block entropy allows us to distinguish between two quantum phases in the system (one critical and the other non-critical) and thus to discern the appearance of a phase transition as we increase the tunneling of the particles. This is deduced from the fact that the entropy changes its behavior (saturate-diverge) when we increase the value of t/W. In this case, considering that the system density is an integer and that we are facing a non-critical phase, the results suggest that the system could be found to be in a Mott-insulator phase characterized by having a finite-correlation length. This would explain the fact that the block entropy increases and saturates rapidly at a constant value. On the contrary, in the critical region, the system could exhibit a superfluid state, characterized by a divergent behavior of the von Neumann block entropy and the delocaliza-

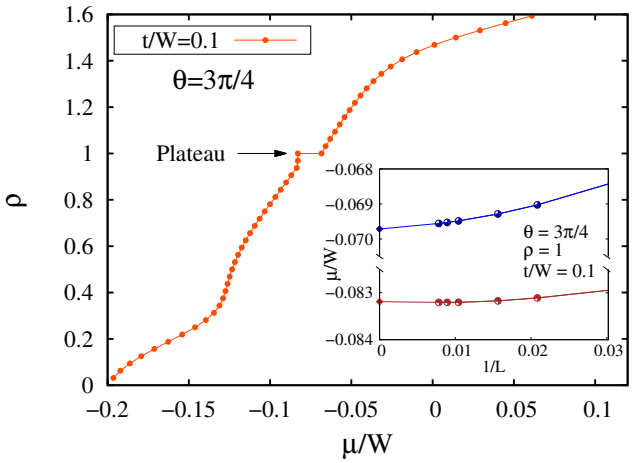

FIG. 3. Global density ρ versus the chemical potential μ/W for $t/W = 0.1$ and a statistical angle $\theta = 3\pi/4$. The system exhibits a Mott plateau at integer density $\rho = 1$. Inset: System size dependence on the chemical potential of anyons with three-body interactions for statistical angle $\theta = 3\pi/4$ and $\rho = 1$. The upper set data correspond to the particle excitation energy and the lower to the hole excitation energy (the lines are visual guides). The values for $1/L = 0$ (diamonds) correspond to an extrapolation to the thermodynamic limit.

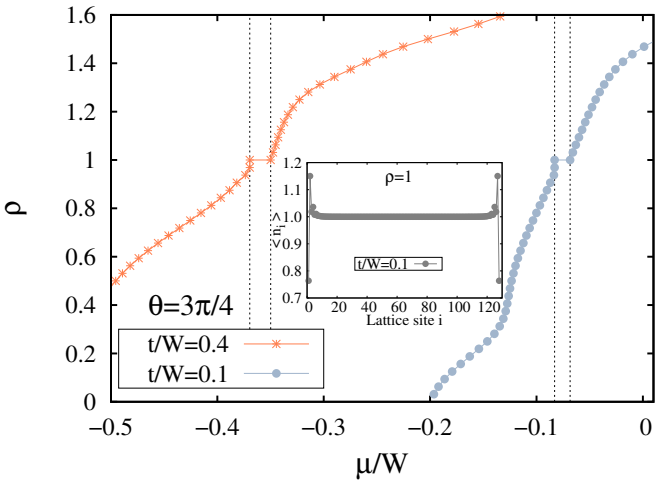

FIG. 4. Global density ρ as a function of the chemical potential μ/W at the thermodynamic limit. Here, we fix the statistical angle to $\theta = 3\pi/4$ and consider $t/W = 0.1$ and $t/W = 0.4$. The vertical dashed lines delimit the insulator phases. In the inset, we show the density profile along the lattice for $\theta = 3\pi/4$, $t/W = 0.1$ and $L = 120$.

tion of the particles along the lattice. In conclusion, for a fixed global density ρ, the anyon-Hubbard model with local three-body interactions exhibits a Mott insulator to superfluid transition for a finite value of t/W.

The phase diagram of anyons in one dimension under two-body interactions shows Mott lobes surrounded by superfluid regions, with the Mott areas decreasing as the global density grows. In particular, it was found that the critical point for a statistical angle $\theta = \pi/4$ and a fixed global density $\rho = 3$ is located at $t/U = 0.172$, $U = 1$ being the strength of the two-body interactions and the energy scale for this case [25, 28]. In Fig. 1, we observe that the Mott lobe for $\rho = 3$ survives for values greater than $t/W = 0.2$, which indicates that the Mott lobes with three-body interactions will be larger than the lobes with two-body interactions, indicating that three-body interactions generate a larger localization in the system, in accordance with previous results for bosons with three-body interactions.

We found that the Hamiltonian problem (2) exhibits Mott and superfluid states, which are characterized by the presence or the lack of an excitation gap at the thermodynamic limit. For a lattice with finite size, the excitation gap is $\Delta\mu(L) = \mu^p(L) - \mu^h(L) = E_0(L, N + 1) + E_0(L, N - 1) - 2E_0(L, N)$, where $E_0(L, N)$ denotes the ground-state energy for L sites and N particles. In particular, a Mott-insulator phase is characterized by the presence of a positive gap at the thermodynamic limit, since the global density is an integer, while the superfluid phase is characterized by the fact that no gap exists at the thermodynamic limit. In Fig. 2, we show the thermodynamic limit values of the chemical potential of adding (μ^p) and removing (μ^h) a particle as a function of the hopping for a statistical angle $\theta = \pi/4$ and different global densities ρ. As is well known, the gapped regions are surrounded by superfluid (gapless) ones, and we obtained that upon increasing the global density, the insulator lobes increase and the position of the critical points moves to greater values of t/W in a manner similar to the boson problem ($\theta = 0$) [47], but for anyons the critical points are greater than for bosons. These results indicate that the three-body interaction and the statistics favor the localization of particles and that greater kinetic energy is required to delocalize the particles and generate superfluid states. Another characteristic of Fig. 2 is the absence of the insulator region for $\rho = 1$, which is due to the fact that the quantum fluctuations, having on average only one particle per site ($\rho = 1$) and $\theta = \pi/4$, are insufficient for generating particle localization. The elongated shape of the Mott-insulator lobes indicates that the gap closes slowly and possibly follows a Kosterlitz-Thouless formula [28]. The length of the Mott regions on the vertical axis at $t/W = 0$ varies with the density of the system. It is notable that for the Bose- and anyon-Hubbard models with two-body interaction, this length does not change with the density. Rather, it is constant and equal to one in the scale of μ/U. When we consider three-body interactions, the length of the lobe with global density ρ at $t/W = 0$ is $\rho - 1$ for both bosons and anyons with $\theta = \pi/4$.

One of the main findings in the anyon-Hubbard model is that the statistics favor the localization of the particles, which is reflected in the increase in the area of the Mott lobes as the statistical angle θ tends toward π [25]. The absence of the $\rho = 1$ Mott insulator lobe in spinless or spinor bosons chains under local three-body in-

teractions is a very well-known result, but in the present paper, our subject of study consist of anyons, and we expected that the statistical angle would generate new findings. Hence we wanted to explore if for $\theta > \pi/4$ new insulator phases can appear. Taking into account the above, we fix the statistical angle to $\theta = 3\pi/4$ and study the evolution of the chemical potential as the number of anyons increases. This leads us to Fig. 3, where we show the global density as a function of the chemical potential at the thermodynamic limit. Note that as we increase the overall density of the system, the chemical potential increases for all the non-integer densities, but for a global density $\rho = 1$ a plateau appears, which indicates the existence of a finite gap at the thermodynamic limit for this density given by the width of the plateau. In the inset of Fig. 3, we show the evolution of the energies for adding (μ^p) and removing (μ^h) particles versus the inverse of the lattice size for anyons with $\theta = 3\pi/4$ and density $\rho = 1$. This evolution is quadratic for $t/W = 0.1$, and at the thermodynamic limit we obtain $\Delta\mu/W = lim_{L,N\to\infty}[\mu^p(L) - \mu^h(L)] = 0.0135$, which corresponds to the width of the plateau and allows us to conclude that the ground state for $\theta = 3\pi/4$ and $\rho = 1$ is an insulator.

Fixing the hopping parameter to $t/W = 0.1$, we can compare Figs. 2 and 3 and observe that the quantum fluctuations are very small for $\theta = \pi/4$. Therefore, the interaction term is unimportant and the ground state is a superfluid (gapless), and the first insulator state is obtained for a global density of $\rho = 2$. However, as the statistical angle increases, the particles are more localized, the effect of the interaction term grows, and an insulator state is obtained for $\rho = 1$. The above insulator state is surrounded by gapless regions (see Fig. 3), but we note that the evolution is different for values greater than or less than $\rho = 1$, and also for $\rho < 1$ two diverse regions can be identified, which indicates that the increase of the statistical angle enriches the superfluid regions.

Up to this point, we have found that the statistics generate an insulator state at a global density $\rho = 1$ from a finite value of θ, but we haven't determined other characteristics of this insulator state. To do this, we calculate the density profile of the particles along a lattice of $L = 120$ with $\theta = 3\pi/4$ and $t/W = 0.1$ (see inset Fig. 4). At the ends of the lattice, we note strong fluctuations due to the open boundary conditions considered in our study. Despite this, we obtain that at each site there is one particle, i. e. $< n_i >= 1$. This result, as well as the fact that there is a finite gap at the thermodynamic limit, allows us to conclude that the ground state is a Mott insulator, which is generated by the statistics, because for spinless and spinor bosons under local three-body interactions it is impossible to obtain a Mott insulator lobe with $\rho = 1$. To distinguish the Mott regions from the superfluid ones, we draw vertical lines in Fig. 4, which shows the global density as a function of the chemical potential at the thermodynamic limit for $\theta = 3\pi/4$ and two different values of the hopping $t/W = 0.1$ and $t/W = 0.4$. From this figure

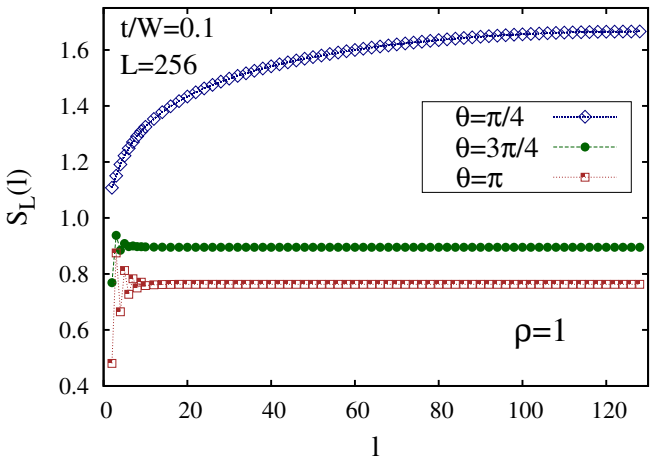

FIG. 5. The von Neumann block entropy $S_L(l)$ as a function of l for a system with size $L = 256$, $\rho = 1$ and $t/W = 0.1$. Here we consider three different values of statistical angle: $\theta = \pi/4$, $\theta = 3\pi/4$, and $\theta = \pi$. The statistical angle drives a quantum phase transition.

it is clear that a quantum phase transition from a Mott insulator to a superfluid phase will take place, and we observe that for both values of t/W the compressibility ($\kappa = \partial\rho/\partial\mu$) is always greater than zero, which indicates the absence of a first-order transition. Also, we obtained that the overall behavior of the global density as a function of μ/W is the same for both values of the hopping. However, the Mott gap is obviously larger at $t/W = 0.4$ than at $t/W = 0.1$. This unusual result can be understood by taking into account that for generating a Mott insulator state with $\rho = 1$ under local three-body interactions, we need the interaction term to be important. For this, the quantum fluctuations must grow, which is caused by the hopping, and with the localization due to the statistics we obtain a larger interaction term, and finally the Mott gap increases with the hopping.

Previously, we showed that the behavior of the block von Neumann entropy allows us to distinguish between critical and noncritical ground states, for instance superfluid and Mott insulator states. With respect to the appearance of insulator states for larger values of the statistical angle, we want to verify the above results by means of the calculation of block entropy (5). We present the results in Fig. 5 for three different values of the angle, $\theta = \pi/4$, $\theta = 3\pi/4$, and $\theta = \pi$, setting the tunneling at $t/W = 0.1$, the global density at $\rho = 1$ and the lattice size at $L = 256$. For $\theta = \pi/4$, we observe that the entropy always increases until it diverges, which indicates that the system is in a superfluid phase. This is consistent with our previous results, in which a non-insulator region was found for this angle and this density (Fig. 2). On the other hand, the above behavior of the block entropy changes for larger values of θ. Specifically, we observe that the block entropy increases very quickly exhibiting an oscillator behavior for small values of the

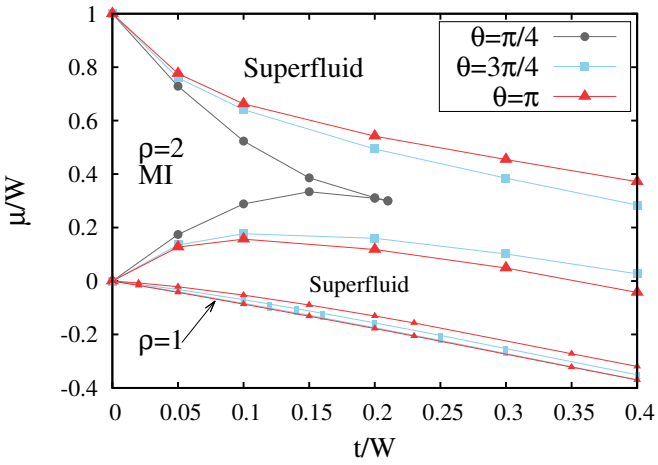

FIG. 6. Phase diagram of the anyon-Hubbard model with local three-body interactions for $\theta = \pi/4$, $3\pi/4$, and π. Mott lobes and a superfluid phase were found, and their boundaries are marked by points that are extrapolations to the thermodynamic limit from DMRG data. The lines are visual guides.

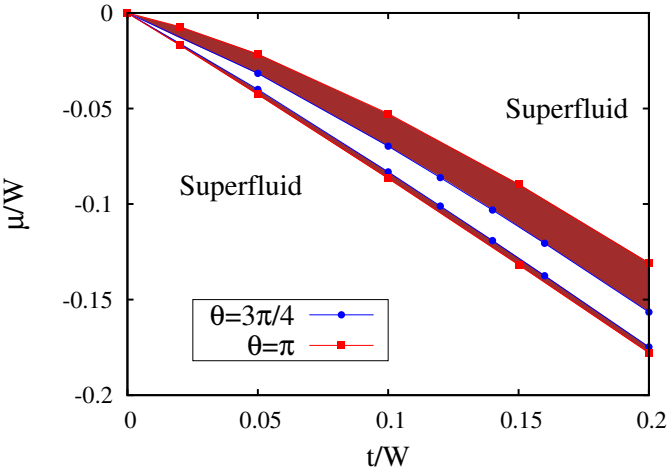

FIG. 7. The $\rho = 1$ Mott lobe at the thermodynamic limit for a statistical angle $\theta = 3\pi/4$ and $\theta = \pi$. The lines are visual guides.

block size, but the range increases with the angle. We cannot explain this oscillator behavior, which is due to the statistics. After the short oscillation, the block entropy remains constant, showing that the system has a finite correlation length. Hence the ground state is a Mott insulator one. Another interesting fact is that the overall value of the von Neumann block entropy diminishes as the statistical angle grows, which indicates that the entanglement decreases. The above discussion allows us to conclude that the statistical angle θ drives a quantum phase transition from a superfluid to a Mott-insulator phase with $\rho = 1$.

We found that the statistics induce a Mott insulator region for larger values of the angle θ. This fact suggests that the phase diagram changes with the statistical angle, and we have to calculate this for statistical angles greater than $\theta = \pi/4$. In Fig. 6, we also draw the results for $\theta = \pi/4$ shown in Fig. 2, in order to compare them with the new results obtained, $\theta = 3\pi/4$ and $\theta = \pi$. We want to emphasize the absence of the $\rho = 1$ Mott lobe for $\theta = \pi/4$. At the atomic limit ($t/W = 0$), we observe that the Mott lobe regions are given by $\mu/W = \rho - 1$ regardless of the statistical angle; hence there is no Mott lobe with $\rho = 1$ at this limit. For the nonzero hopping parameter, we see that the Mott lobe with $\rho = 2$ decreases as t/W grows, a fact that is maintained for any angle; however, it is clear that as the angle grows the statistics favor the localization of the particles, which is reflected in the increase of the Mott lobe area and the displacement of the critical point towards larger values. The phase diagram shows a much smaller $\rho = 2$ Mott lobe than the anyon chain with two-body interactions. Also, we obtained a re-entrant behavior for the $\rho = 2$ Mott lobe regardless of the statistical angle, i. e. for a fixed chemical potential value the ground state passes from a Mott insulator to a superfluid phase and then returns to the Mott insulator one. Note that this does not happen for the $\rho = 1$ Mott lobe (see Fig. 7). The emergence and evolution of the $\rho = 1$ Mott lobe as the hopping parameter increases is shown Fig. 7 for two different angles $\theta = 3\pi/4$ and $\theta = \pi$, where a zoom in has been made. From this it is clear that if the statistics increase, the localization grows. Note that for negative constant values of the chemical potential, the ground state is a superfluid with density lower than one. As the kinetic energy increases, it goes to a Mott insulator state with $\rho = 1$ and finally returns to a superfluid state, but with a density greater than one. From this figure, it is clear that the Mott lobe area increases with the hopping.

We showed that the statistical angle drives a quantum phase transition from a superfluid state to a Mott insulator one in the range of $\theta = \pi/4$-$3\pi/4$ for a fixed hopping parameter $t/W = 0.1$ and global density $\rho = 1$ (see Fig. 5). However a pending task is to explore the ground state phase diagram as a function of the statistical angle, which is shown in Fig. 8 for three different values of the hopping parameter, $t/W = 0.1$, 0.15, and 0.20. We obtain that there is a critical value of the angle at which the Mott insulator phase appears, and this critical value moves to greater values as the hopping grows. A reentrance phase transition was observed, since the hole excitation energy curve exhibits a maximum. Hence at some suitable constant chemical potential, the model displays a sequence of quantum phase transitions between the Mott insulator and the superfluid phases. In the sequence (from left to right), we have a change from a superfluid region with $\rho > 1$ to a Mott insulator one with $\rho = 1$ and then again to an superfluid region ($\rho < 1$), and finally the system remains in an insulator state. Finally, we note that for a fixed angle, the Mott lobe area increases with the tunneling. Note that the shape of the Mott lobes around the critical point is not elongated like others shown in Fig.

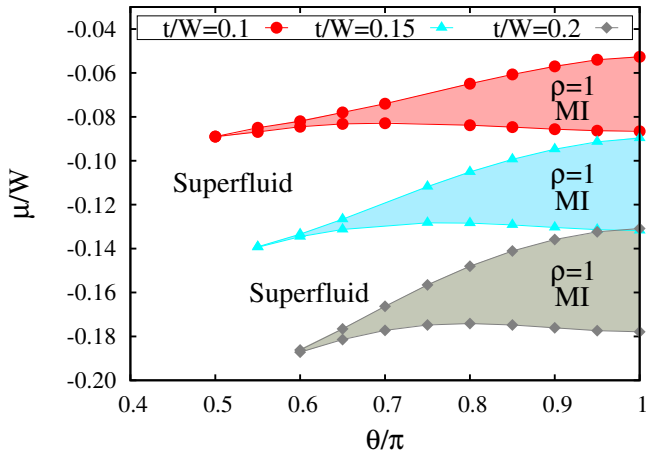

FIG. 8. Phase diagram of the anyon-Hubbard model with local three-body interactions in the plane $(\mu/W, \theta/\pi)$. We consider three different hopping parameters $t/W = 0.1, 0.15$ and 0.2. The points are extrapolations to the thermodynamic limit from DMRG data and the lines are visual guides. MI means Mott insulator regions.

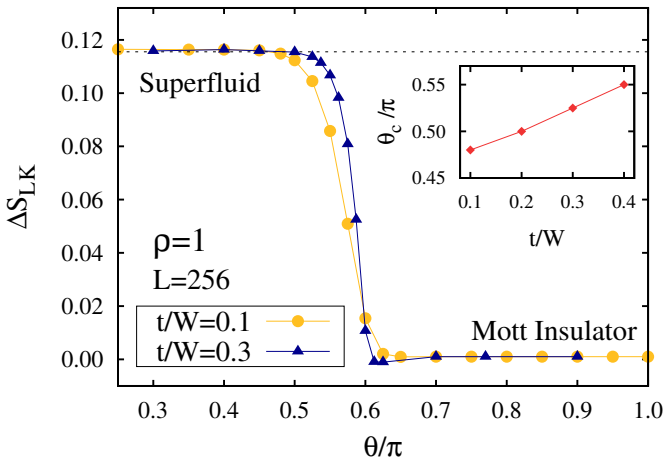

FIG. 9. The estimator ΔS_{LK} as a function of angle θ for $t/W = 0.1$ and $t/W = 0.3$. Here we fixed L=256 and $\rho = 1$. The points are DMRG data and the lines are a visual guide. Inset: Evolution of the critical angle θ_c with the hopping parameter.

2 or others reported previously, which can indicate that this quantum phase transition is not of the Kosterlitz-Thouless type.

It is well known in the literature that using the gap vanishing point to determine the critical point related to a quantum phase transition gives us poor results and that some measures of the entanglement can help us in this task. Precisely, it has been shown that for models like the Bose-Hubbard one, the estimator based on the von Neumann block entropy $\Delta S_{LK}(L) = S_L(L/2) - S_{L/2}(L/4)$ proposed by Laüchli and Kollath leads to better results [48]. According to above definition and the expression Eq. (5), we obtain:

$$\Delta S_{LK}(L) = \begin{cases} \frac{c}{6} ln[2], & \theta \leq \theta_c, \\ 0, & \theta > \theta_c, \end{cases} \tag{6}$$

θ_c being the critical angle.

In Fig. 9, the evolution of the estimator ΔS_{LK} with the statistical angle is shown for an anyon chain with $\rho = 1$, and $L = 256$. When $\theta = 0$, the ground state is a superfluid, because the $\rho = 1$ Mott insulator lobe does not exist for bosons under local three-body interactions. Therefore, the estimator will be equal to $ln(2)/6$, and it remains at this point for non-zero values of the statistical angle, indicating that there is a range of values of θ for which the ground state is a superfluid. However, from a given critical angle the estimator collapses to zero within a short range. After that, the estimator remains constant at zero, indicating that the ground state is now a Mott insulator one. Regardless of the hopping parameter, we see that the estimator clearly shows us the quantum phase transition from a superfluid to a Mott insulator state. Note that the superfluid region becomes greater and the shape of the curve becomes sharper as the hopping increases, although at the thermodynamic limit the shape of the curve will be a step function, according to the expression Eq. (6). The critical point corresponds to the greatest value of θ, for which the estimator is equal to $ln(2)/6$, and we obtain that the position of the critical angle moves to greater values as the hopping grows (see inset of Fig. 9).

C. Conclusions

We studied the interplay of multi-body interactions and the statistics in an anyon-Hubbard model, which was mapped to a modified Bose-Hubbard model by means of a fractional Jordan-Wigner transformation. This last-named model was explored using the density matrix renormalization group method, and we found that the model exhibits superfluid and Mott insulator regions in the phase diagram. The expression $\mu/W = \rho - 1$ determines the width of the Mott lobes at the atomic limit, regardless of the statistics. As in the spinless and spinor boson cases, we obtain that for small statistical angles there is no Mott insulator region with density $\rho = 1$ when local three-body interactions are considered. However the above Mott insulator state emerges as the statistics grow, this fact being one of the main findings of this study.

We found that the statistics drive a quantum phase transition from a superfluid phase to a Mott insulator one when the density is $\rho = 1$. This quantum phase transition was clearly identified by means of the von Neumann block entropy and the estimator proposed by Laüchli and Kollath [48]. Using the latter to estimate the critical angles, we see that the hopping parameter moves the critical angles to greater values.

The superfluid regions are modified by the statistics.

This is evident in the curve of the global density as a function of the chemical potential, where three different superfluid regions can be distinguished (Fig. 3). These superfluid regions resemble ones obtained by Zhang and co-workers [29], who studied the pseudo-anyon Hubbard model in one dimension. For densities lower than $\rho = 1$, we believe that our first superfluid region ($0 < \rho \lesssim 0.34$) corresponds to the superfluid phase SF_0, and the second one ($0.34 \lesssim \rho < 1$) could be related to a separation of phases (PS). For $\rho > 1$, our results suggest that the superfluid is of the SF_π type, but we did not find evidence of the presence of paired phases (PP). We calculated the chemical potential at the thermodynamic limit as a function of the global density at the pseudo-fermion limit $\theta = \pi$ for $t/W = 0.1$ (not shown), and found that the curve is very similar to Fig. 10 of reference [29], but with the absence of the paired phases. We will explore the superfluid regions of the anyon-Hubbard model under local three-body interactions in a future study.

ACKNOWLEDGMENTS

The authors are thankful for the support of DIEB-Universidad Nacional de Colombia and COLCIENCIAS (grant No. FP44842-057-2015). Silva-Valencia and Franco are grateful for the hospitality of the ICTP, where part of this work was done.

[1] J. M. Leinaas and J. Myrheim, Il Nuovo Cimento B **37**, 1 (1977).
[2] F. Wilckzek, Phys. Rev. Lett. **49**, 957 (1982).
[3] F. D. M. Haldane, Phys. Rev. Lett. **67**, 937 (1991).
[4] D. C. Tsui, H. Stormer, and J. Gossard, Phys. Rev. Lett. **48**, 1559 (1982).
[5] R. B. Laughlin, Phys. Rev. Lett. **50**, 1395 (1983).
[6] B. I. Halperin, Phys. Rev. Lett. **52**, 1583 (1984).
[7] F. E. Camino, W. Zhou, and V. J. Goldman, Phys. Rev. B **72**, 075342 (2005).
[8] A. Y. Kitaev, Ann. Phys. **303**, 2 (2003).
[9] C. Nayak, S. H. Simon, A. Stern, M. Freedman, and S. D. Sarms, Rev. Mod. Phys. **80**, 1083 (2008).
[10] J. Alicea, Y. Oreg, G. Rafael, F. von Oppen, and M. P. A. Fisher, Nat. Phys. **7**, 412 (2011).
[11] A. Kundu, Phys. Rev Lett. **83**, 1275 (1999).
[12] M. Batchelor, X.-W. Guan, and N. Oelkers, Phys. Rev Lett. **96**, 210402 (2006).
[13] P. Calabrese and M. Mintchev, Phys. Rev. B **75**, 233104 (2007).
[14] Y. Hao and S. Chen, Phys. Rev. A **86**, 043631 (2012).
[15] O. I. Patu, J. Stat. Mech. **2015**, P01004 (2015).
[16] N. T. Zinner, Phys. Rev. A **92**, 063634 (2015).
[17] C. Vitoriano, Phys. Rev. Lett. **102**, 146404 (2009).
[18] M. D. Girardeau, Phys. Rev. Lett. **97**, 100402 (2006).
[19] B. Paredes, P. Fedichev, J. I. Cirac, and P. Zoller, Phys. Rev. Lett. **87**, 010402 (2001).
[20] L.-M. Duan, E. Demler, and M. D. Lukin, Phys. Rev. Lett. **91**, 090402 (2003).
[21] L. Jiang, G. K. Brennen, A. V. Gorshkov, K. Hammerer, M. Hafezi, E. Demler, M. D. Lukin, and P. Zoller, Nat. Phys. **4**, 482 (2008).
[22] M. Aguado, G. K. Brennen, F. Verstraete, and J. I. Cirac, Phys. Rev. Lett. **101**, 260501 (2008).
[23] S. Longhi and G. D. Valle, Optics Letters **37**, 2160 (2012).
[24] Y. Zhang, G. J. Sreejith, and J. K. Jain, Phys. Rev. B **92**, 075116 (2015).
[25] T. Keilmann, S. Lanzmich, I. McCulloch, and M. Roncaglia, Nat. Commun. **2**, 361 (2011).
[26] S. Greschner and L. Santos, Phys. Rev. Lett. **115**, 053002 (2015).
[27] C. Sträter, S. C. L. Srivastava, and A. Eckardt, Phys. Rev. Lett. **117**, 205303 (2016).
[28] J. Arcila-Forero, R. Franco, and J. Silva-Valencia, Phys. Rev. A **94**, 013611 (2016).
[29] W. Zhang, S. Greschner, E. Fan, T. C. Scott, and Y. Zhang, (2016), ArXiv:1609.02594.
[30] G. Tang, S. Eggert, and A. Pelster, New J. Phys. **17**, 123016 (2015).
[31] G. Marmorini, M. Pepe, and P. Calabrese, J. Stat. Mech. **2016**, 073106 (2016).
[32] F. Lange, S. Ejima, and H. Fehske, (2016), ArXiv:1612.00605.
[33] E. Duchon, Y. L. Loh, and N. Trivedi, (2013), ArXiv:1311.0543.
[34] M. Greiner *et al.*, Nature **419**, 51 (2002).
[35] S. Will, T. Best, U. Schneider, L. Hackermüller, D.-S. Lühmann, and I. Bloch, Nature **465**, 197 (2010).
[36] R. Ma, M. E. Tai, P. M. Preiss, W. S. Bakr, J. Simon, and M. Greiner, Phys. Rev. Lett. **107**, 095301 (2011).
[37] J. Silva-Valencia and A. M. C. Souza, Phys. Rev. A **84**, 065601 (2011).
[38] J. Silva-Valencia and A. M. C. Souza, Eur. Phys. J. B **85**, 161 (2012).
[39] A. J. Daley and J. Simon, Phys. Rev. A **89**, 053619 (2014).
[40] T. Sowiński, Cent. Eur. J. Phys. **12**, 473 (2014).
[41] H.-N. Dai, B. Yang, A. Reingruber, H. Sun, X.-F. Xu, Y.-A. Chen, Z.-S. Yuan, and J.-W. Pan, (2016), ArXiv:1602.05709v1.
[42] L. Amico, R. Fazio, A. Osterloh, and V. Vedral, Rev. Mod. Phys. **80**, 517 (2008).
[43] R. Islam, R. Ma, P. M. Preiss, M. E. Tai, A. Lukin, M. Rispoli, and M. Greiner, Nature **528**, 77 (2015).
[44] P. Calabrese and J. Cardy, J. Stat. Mech. **2004**, P06002 (2004).
[45] Ö. Legeza, J. Roder, and B. A. Hess, Phys. Rev. B **67**, 125114 (2003).
[46] J. Carrasquilla, S. R. Manmana, and M. Rigol, Phys. Rev. A **87**, 043606 (2013).
[47] C. A. Avila, R. Franco, A. M. C. Souza, M. S. Figueira, and J. Silva-Valencia, Phys. Lett. A **378**, 3233 (2014).
[48] A. M. Läuchli and C. Kollath, J. Stat. Mech. **2008**, P05018 (2008).